One-Pot Synthesis of Pd Nanoparticles Supported on Carbide-Derived Carbon for Oxygen Reduction Reaction

Madis Lüsi[1], Heiki Erikson[1], Maike Käärik[1] Helle-Mai Piirsoo[2], Jaan Aruväli[3], Arvo Kikas[2], Vambola Kisand[2], Jaan Leis[1], Kaupo Kukli[2], Kaido Tammeveski[1,*]

[1]*Institute of Chemistry, University of Tartu, Ravila 14a, 50411 Tartu, Estonia*
[2]*Institute of Physics, University of Tartu, W. Ostwald Str. 1, 50411 Tartu, Estonia*
[3]*Institute of Ecology and Earth Sciences, University of Tartu, Vanemuise 46, 51014 Tartu, Estonia*

*Corresponding author. Tel.: +372 7375168; E-mail: kaido.tammeveski@ut.ee (K. Tammeveski)

Pore size distribution (PSD) of CDC materials

Table S1. Texture characteristics of CDC materials measured using standard methodology [1].

Sample	Precursor	SSA_{BET} ($m^2\ g^{-1}$)	S_{dft} ($m^2\ g^{-1}$)	V_{mic} ($cm^3\ g^{-1}$)	V_{tot} ($cm^3\ g^{-1}$)	S_{dft} mic ($m^2\ g^{-1}$)	S_{dft} meso ($m^2\ g^{-1}$)
CDC-1	TiC-PT with steam	2080	1803	0.84	1.1	1701	102
CDC-2	B_4C	1588	1386	0.55	1.13	1076	1385
CDC-3	TiCN 50/50	838	828	0.26	0.94	593	828

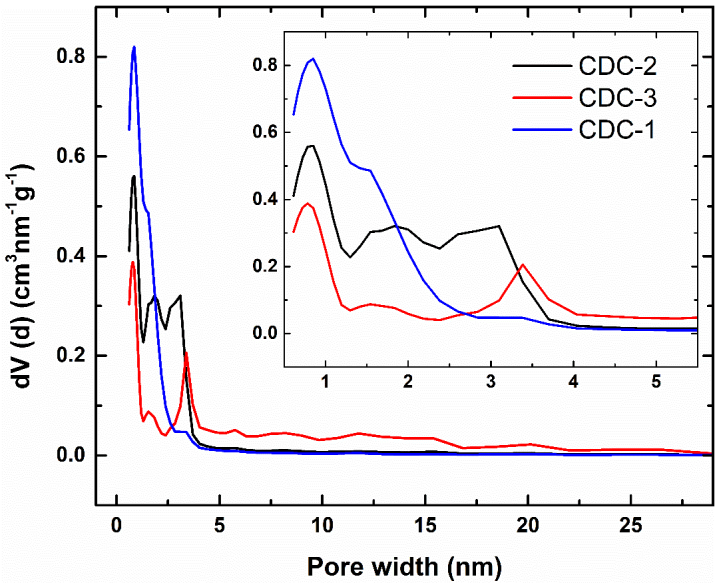

Figure S1. PSD graph of CDC materials.

Pd particle size distribution

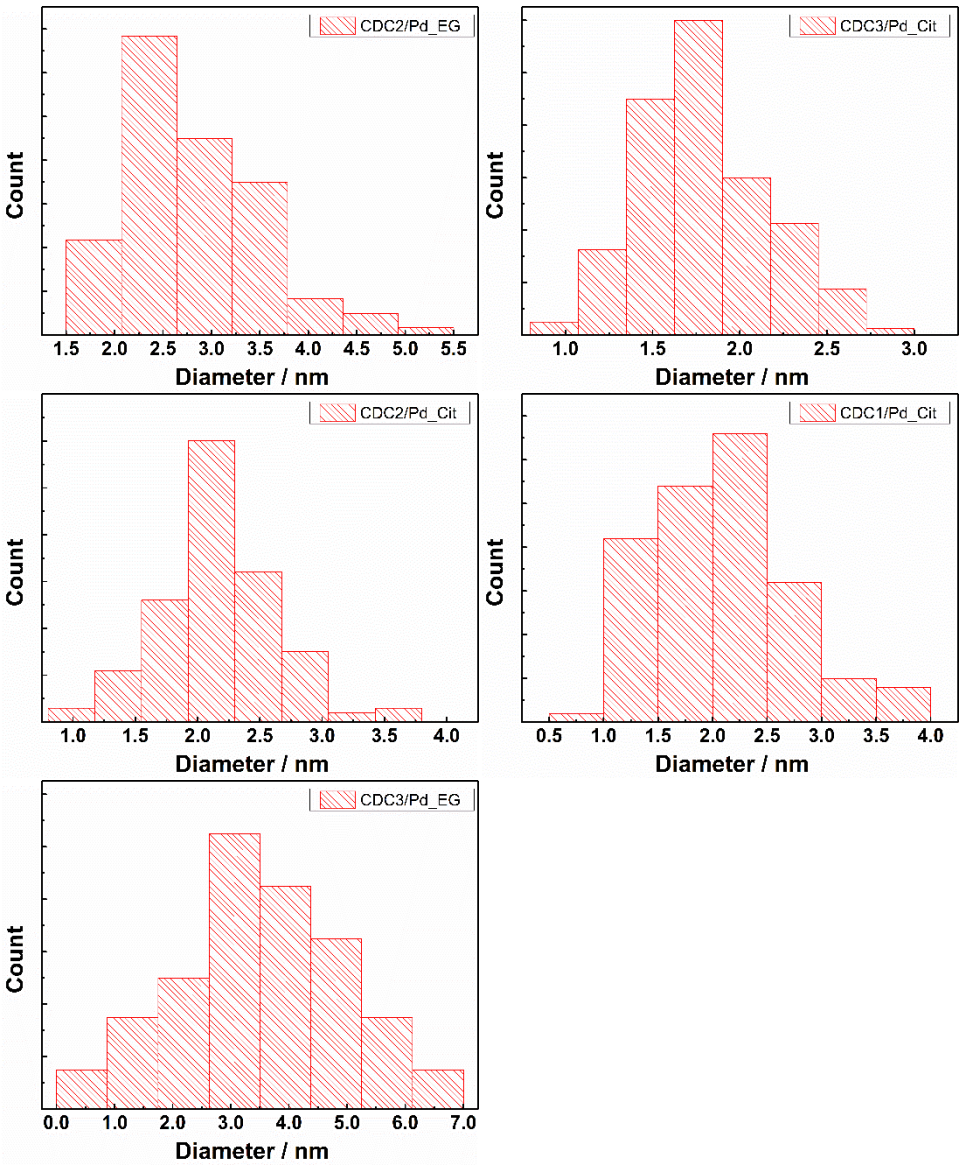

Figure S2. Particle size distribution for catalyst materials.

Elemental mapping of CDC3 materials

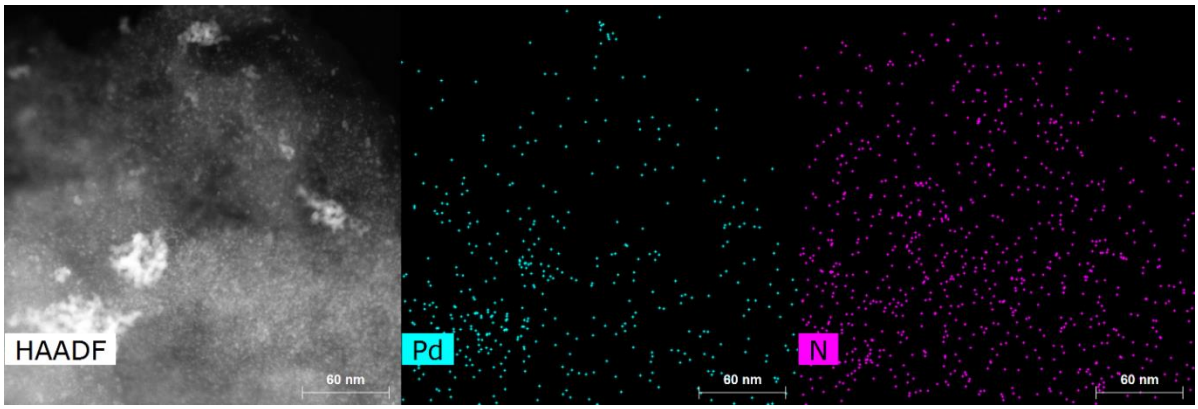

Figure S3. STEM and elemental mapping of CDC3/Pd_Cit.

XPS analysis

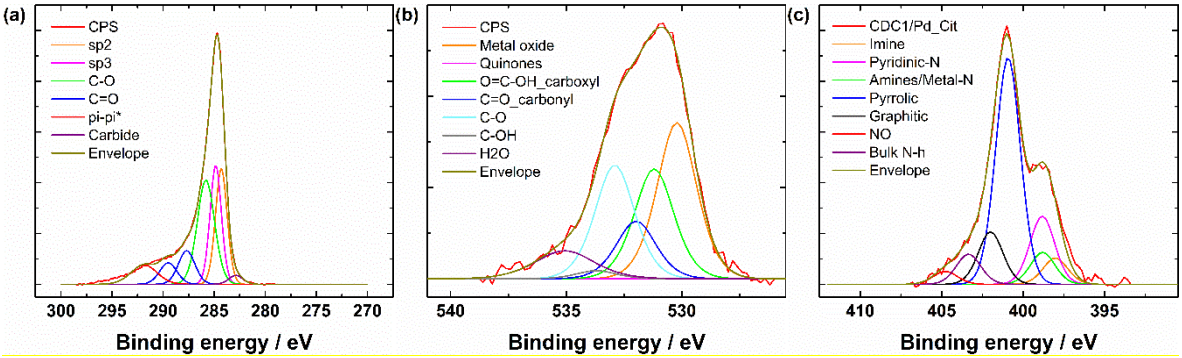

Figure S4. a) C1s, b) O1s, and c) N1s XPS spectra for CDC3.

Table S2. Components of CDC3.

C1s	at%	O1s	at%	N1s	at%
sp2	20.02	metal oxide	1.02	Imine	0.38
sp3	20	quinones	0	Pyridinic-N	0.98
C-O	26.93	O=C-OH carboxyl	0.72	Amines/Metal-Nx	0.46
C=O	5.59	C=O carbonyl	0.38	Pyrrolic	3.27
C=O	8.3	C-O	0.74	Graphitic	0.76
pi-pi*	7.61	C-OH	0.05	NO	0.19
carbide	1.9	Water, chemisorbed O	0.28	bulk N-h	0.44

Table S3. Pd species in catalyst materials.

Catalyst	PdO (at%)	PdO_2 (at%)	Pd (at%)	Pd plasmon (at%)
CDC1/Pd_Cit	0.8	0.28	0.77	0.12
CDC2/Pd_Cit	0.49	0.2	0.47	0.06
CDC3/Pd_Cit	0.97	0.45	1.05	0.13
CDC2/Pd_EG	0.45	0.17	0.6	0.05
CDC3/Pd_EG	0.33	0.1	0.3	0.05

Cyclic voltammetry

CV curves measured before and after CO-stripping and after ORR experiments named CV1, CV2, and CV3, respectively.

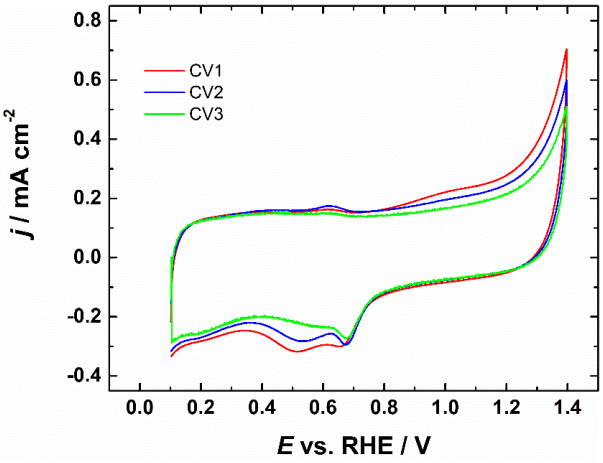

Figure S5. CV curves of CDC1/Pd_Cit catalyst in Ar-saturated 0.1 M KOH solution, v = 50 mV s^{-1}.

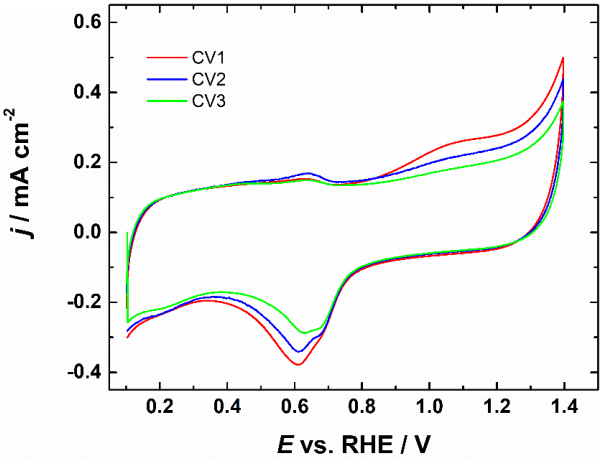

Figure S6. CV curves of CDC2/Pd_Cit catalyst in Ar-saturated 0.1 M KOH solution, v = 50 mV s^{-1}.

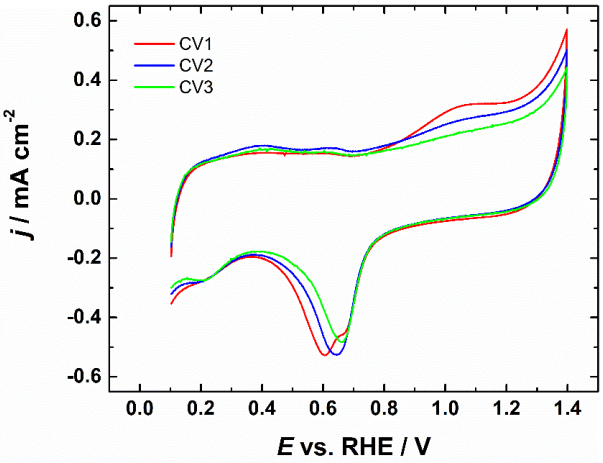

Figure S7. CV curves of CDC3/Pd_Cit catalyst in Ar-saturated 0.1 M KOH solution, v = 50 mV s^{-1}.

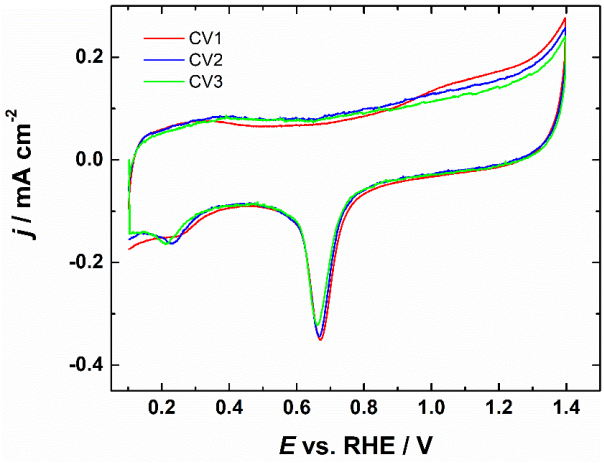

Figure S8. CV curves of CDC2/Pd_EG catalyst in Ar-saturated 0.1 M KOH solution, v = 50 mV s^{-1}.

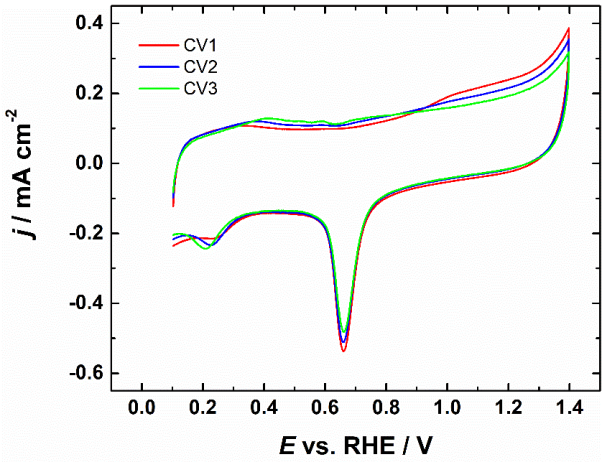

Figure S9. CV curves of CDC3/Pd_EG catalyst in Ar-saturated 0.1 M KOH solution, v = 50 mV s^{-1}.

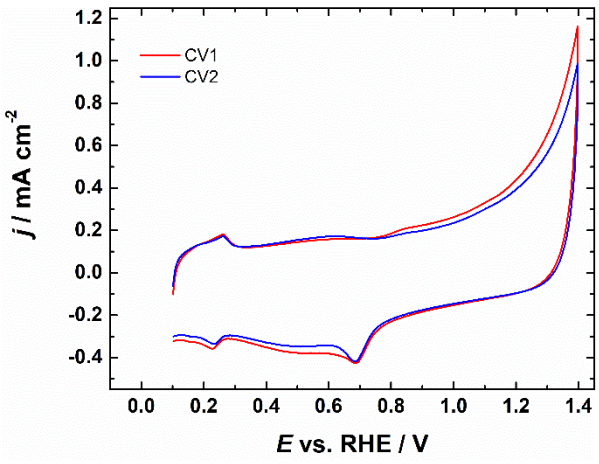

Figure S10. CV curves of CDC1/Pd_Cit catalyst in Ar-saturated 0.5 M H_2SO_4 solution, v = 50 mV s^{-1}

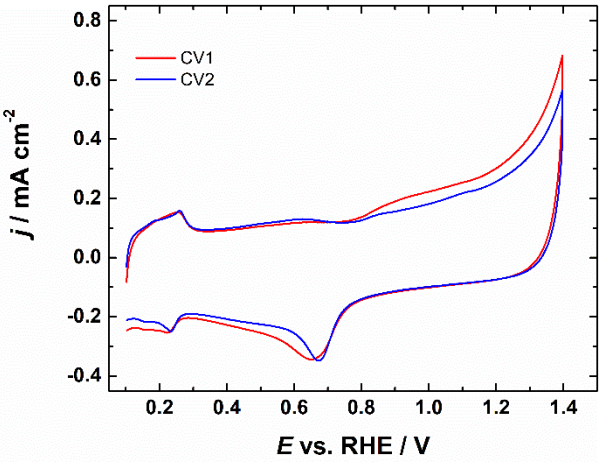

Figure S11. CV curves of CDC2/Pd_Cit catalyst in Ar-saturated 0.5 M H_2SO_4 solution, v = 50 mV s^{-1}

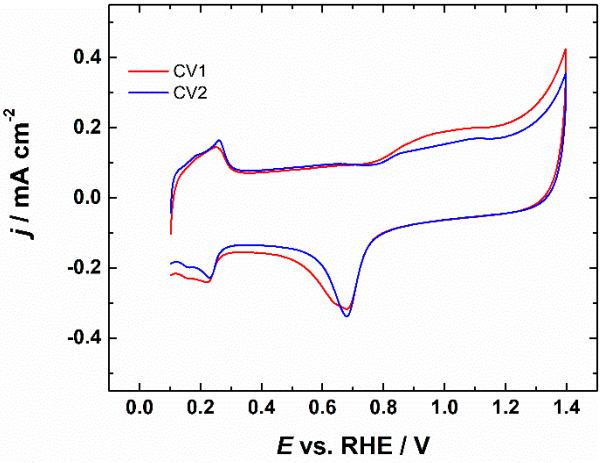

Figure S12. CV curves of CDC3/Pd_Cit catalyst in Ar-saturated 0.5 M H_2SO_4 solution, v = 50 mV s^{-1}

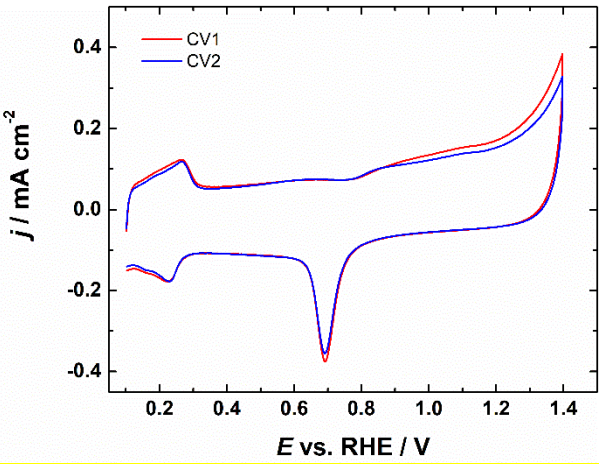

Figure S13. CV curves of CDC2/Pd_EG catalyst in Ar-saturated 0.5 M H_2SO_4 solution, v = 50 mV s^{-1}

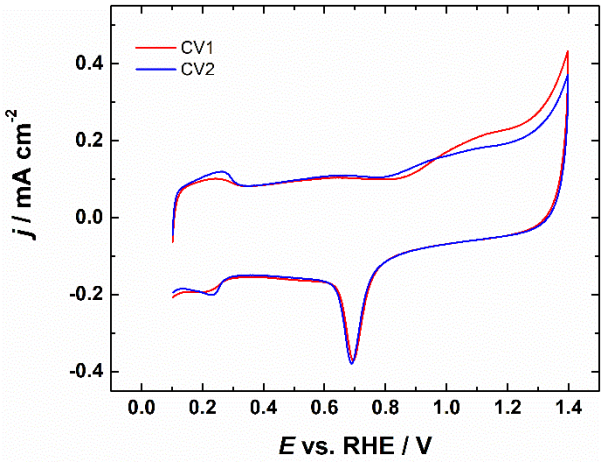

Figure S14. CV curves of CDC3/Pd_EG catalyst in Ar-saturated 0.5 M H_2SO_4 solution, v = 50 mV s^{-1}

ORR studies

RDE polarization data was analyzed using the Koutecky-Levich (K-L) equation:

$$\frac{1}{j} = \frac{1}{j_k} + \frac{1}{j_d} = -\frac{1}{nFkC_{O_2}^b} - \frac{1}{0.62nFD_{O_2}^{2/3}\nu^{-1/6}C_{O_2}^b\omega^{1/2}} \quad \text{(S1)}$$

where j is the overall O_2 reduction current density, j_k represents kinetic and j_d diffusion-limited current densities. k is the electrochemical rate constant for O_2 reduction (cm s^{-1}), n is the number of electrons transferred per O_2 molecule, F is the Faraday constant (96,485 C mol^{-1}) and ω is the rotation rate of the electrode (rad s^{-1}). For O_2-saturated 0.1 M KOH solution these values were used: kinematic viscosity (ν = 0.01 cm^2 s^{-1} [2]), concentration of O_2 (C^b_{O2} = 1.2×10^{-6} mol cm^{-3} [3]), and diffusion coefficient of O_2 (D_{O2} = 1.9×10^{-5} cm^2 s^{-1} [3]).

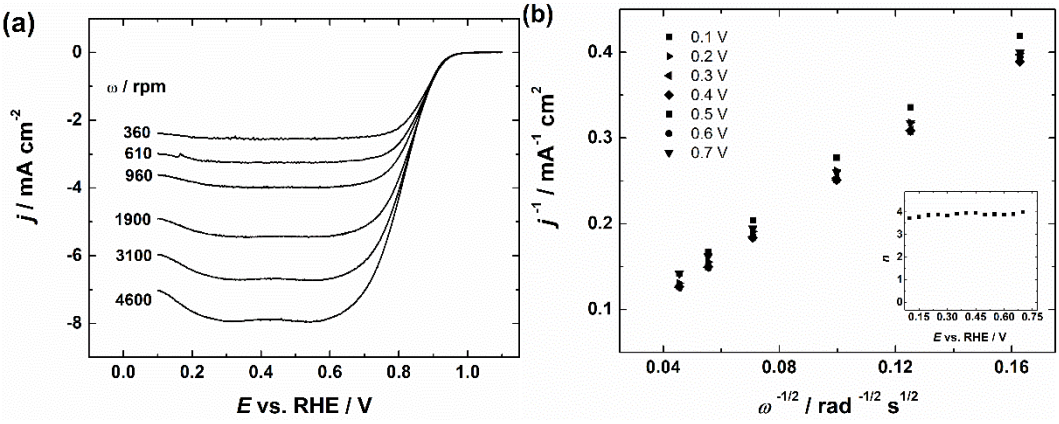

Figure S15. a) RDE results of CDC1/Pd_Cit in O_2-saturated 0.1 M KOH and b) corresponding K–L plots, inset shows the potential dependence of n.

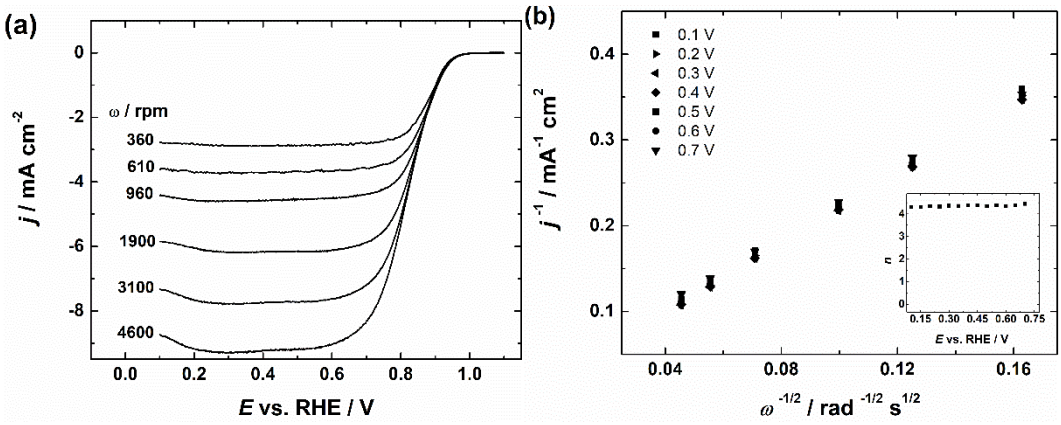

Figure S16. a) RDE results of CDC2/Pd_Cit in O_2-saturated 0.1 M KOH and b) corresponding K–L plots, inset shows the potential dependence of n.

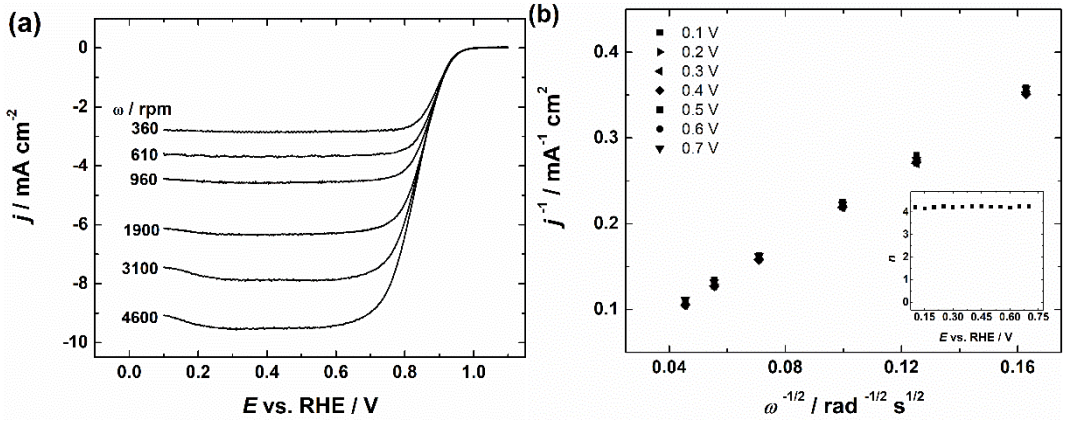

Figure S17. a) RDE results of CDC3/Pd_Cit in O_2-saturated 0.1 M KOH and b) corresponding K–L plots, inset shows the potential dependence of n.

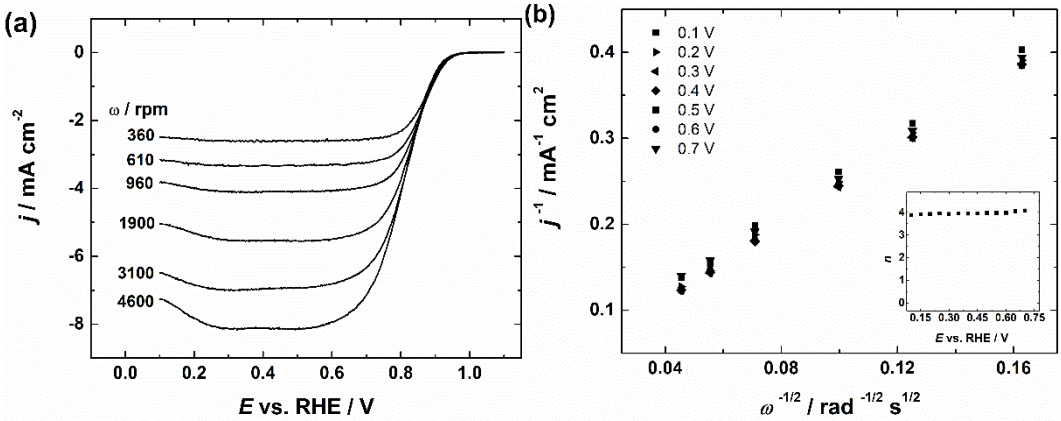

Figure S18. a) RDE results of CDC2/Pd_EG in O_2-saturated 0.1 M KOH and b) corresponding K–L plots, inset shows the potential dependence of n.

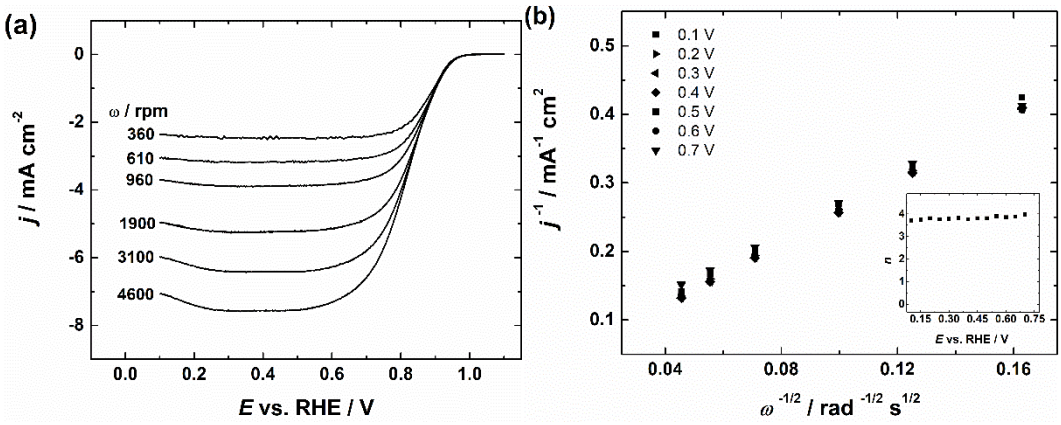

Figure S19. a) RDE results of CDC3/Pd_EG in O_2-saturated 0.1 M KOH and b) corresponding K–L plots, inset shows the potential dependence of *n*.

Table S4. Comparison with various Pd/C materials from literature.

Catalyst	$E_{1/2}$ (V)	SA at 0.9 V (mA cm^{-2})	MA at 0.9 V (A g^{-1})	Reference
CDC2/Pd_Cit	0.844	0.624	289	This work
CDC2/Pd_EG	0.830	0.512	276	This work
h-BN/C/Pd:17	0.91	0.86	250	[4]
Pd/C	0.866	0.130	98	[5]
Pd-B/C	0.883	0.170	145	[5]
Pd/CSN	N/A	0.114	286	[6]
Pd10/nCNF	0.769	N/A	174	[7]
Pd-HCS-700	0.802	N/A	60	[8]
Pd/C	0.868	~0.92	~43	[9]
PdSph-20/C	N/A	~0.15	~101	[10]
Pd/N-HsGY	0.849	~0.33[1]	N/A	[11]
Pd MSs	N/A	~1.25	~440	[12]
Pd/C-400[2]	N/A	~0.20	~104	[13]

[1] Read from a curve. [2] vs 0V Hg/HgO in 0.1M NaOH

References

[1] M. Käärik, M. Arulepp, M. Käärik, U. Maran, J. Leis, Characterization and prediction of double-layer capacitance of nanoporous carbon materials using the Quantitative nano-Structure-Property Relationship approach based on experimentally determined porosity descriptors, Carbon 158 (2020) 494-504.

[2] D.R. Lide, CRC handbook of chemistry, physics, CRC Press, Boca Raton, 2001.

[3] R.E. Davis, G.L. Horvath, C.W. Tobias, The solubility and diffusion coefficient of oxygen in potassium hydroxide solutions, Electrochimica Acta 12(3) (1967) 287-297.

[4] Y. Chen, J. Cai, P. Li, G. Zhao, G. Wang, Y. Jiang, J. Chen, S.X. Dou, H. Pan, W. Sun, Hexagonal Boron Nitride as a Multifunctional Support for Engineering Efficient Electrocatalysts toward the Oxygen Reduction Reaction, Nano Letters 20(9) (2020) 6807-6814.

[5] M. Wang, X. Qin, K. Jiang, Y. Dong, M. Shao, W.-B. Cai, Electrocatalytic Activities of Oxygen Reduction Reaction on Pd/C and Pd–B/C Catalysts, The Journal of Physical Chemistry C 121(6) (2017) 3416-3423.
[6] W. Yan, Z. Tang, L. Li, L. Wang, H. Yang, Q. Wang, W. Wu, S. Chen, Ultrasmall Palladium Nanoclusters Encapsulated in Porous Carbon Nanosheets for Oxygen Electroreduction in Alkaline Media, ChemElectroChem 4(6) (2017) 1349-1355.
[7] M.A. Khalily, B. Patil, E. Yilmaz, T. Uyar, Atomic Layer Deposition of Pd Nanoparticles on N-Doped Electrospun Carbon Nanofibers: Optimization of ORR Activity of Pd-Based Nanocatalysts by Tuning Their Nanoparticle Size and Loading, ChemNanoMat 5(12) (2019) 1540-1546.
[8] X. Wang, Z. Chen, S. Chen, H. Wang, M. Huang, Nitrogen and Oxygen Co-Doping Assisted Synthesis of Highly Dispersed Pd Nanoparticles on Hollow Carbon Spheres as Efficient Electrocatalysts for Oxygen Reduction Reaction, Chemistry – A European Journal 26(55) (2020) 12589-12595.
[9] Y. Yang, G. Chen, R. Zeng, A.M. Villarino, F.J. DiSalvo, R.B. van Dover, H.D. Abruña, Combinatorial Studies of Palladium-Based Oxygen Reduction Electrocatalysts for Alkaline Fuel Cells, Journal of the American Chemical Society 142(8) (2020) 3980-3988.
[10] M. Lusi, H. Erikson, A. Sarapuu, K. Tammeveski, J. Solla-Gullon, J.M. Feliu, Oxygen reduction reaction on carbon-supported palladium nanocubes in alkaline media, Electrochemistry Communications 64 (2016) 9-13.
[11] W. Si, Z. Yang, X. Hu, Q. Lv, X. Li, F. Zhao, J. He, C. Huang, Preparation of zero valence Pd nanoparticles with ultra-efficient electrocatalytic activity for ORR, Journal of Materials Chemistry A 9(25) (2021) 14507-14514.
[12] H. Lv, D. Xu, L. Sun, J. Henzie, S.L. Suib, Y. Yamauchi, B. Liu, Ternary Palladium–Boron–Phosphorus Alloy Mesoporous Nanospheres for Highly Efficient Electrocatalysis, ACS Nano 13(10) (2019) 12052-12061.
[13] L. Jiang, A. Hsu, D. Chu, R. Chen, Size-Dependent Activity of Palladium Nanoparticles for Oxygen Electroreduction in Alkaline Solutions, Journal of the Electrochemical Society 156(5) (2009) B643-B649.